AGU100 ADVANCING EARTH AND SPACE SCIENCE

JGR

Journal of Geophysical Research: Atmospheres

RESEARCH ARTICLE
10.1029/2018JD028432

Special Section:
Water-soil-air-plant-human nexus: Modeling and observing complex land-surface systems at river basin scale

Role of Groundwater in the Dryland Ecohydrological System: A Case Study of the Heihe River Basin

Yingying Yao[1], Yong Tian[2,3], Charles Andrews[2,3], Xi Li[4], Yi Zheng[2,3], and Chunmiao Zheng[2,3,5]

[1]Department of Earth and Environmental Science, School of Human Settlements and Civil Engineering, Xi'an Jiaotong University, Xi'an, China, [2]School of Environmental Science and Engineering, Southern University of Science and Technology, Shenzhen, China, [3]Guangdong Provincial Key Laboratory of Soil and Groundwater Pollution Control, Southern University of Science and Technology, Shenzhen, China, [4]Institute of Water Sciences, College of Engineering, Peking University, Beijing, China, [5]Department of Geological Sciences, University of Alabama, Tuscaloosa, AL, USA

Abstract Groundwater sustains food production and ecosystem health in drylands. Groundwater influences the interlinked hydrological processes and ecological state; however, the function of groundwater in the ecohydrological system is yet to be quantified clearly. In this study, we assess the role of groundwater in the ecohydrological system of the Heihe River Basin, using a regional-scale integrated model with multiple independent databases. Our results show that first, in over 40% of mid-lower plain, the groundwater table is less than 10 m deep, and both recharge and evaporation of groundwater dominate seasonal water budget variations; recharge is more affected by land use than groundwater evaporation, and it has a higher variability ranging over 2 orders of magnitude within vegetated land use type. Second, mountain block recharge maintains the piedmont groundwater; the upper mountainous partition between baseflow and mountain block recharge impacts the evaporation and two-way exchange between groundwater and stream/lake in the downstream alluvial plain. Third, the groundwater system stores over 50% of streamflow in the dry season and about 10% in the wet season along leakage segments; groundwater dominates the streams by contributing about 40% of streamflow in the dry season along the seepage segments of the middle alluvial plain. Fourth, shallow groundwater sustains a vibrant ecosystem directly by providing a stable source of water for vegetation and indirectly by buffering lateral groundwater flow. Our study not only bridges the quantification gap for regional studies of drylands but also provides suggestions on water management and future water sustainability and food security.

Key Points:
- Shallow groundwater (<10 m deep) of alluvial plain responds to land surface regimes and dominates seasonal water budget variations
- Groundwater system in mountainous upstream impacts the evapotranspiration and surface-groundwater interactions in alluvial plain downstream
- Groundwater sustains ecosystem by contributing to evapotranspiration of vegetation in the growing season and buffering lateral flow

Correspondence to:
C. Zheng,
zhengcm@sustc.edu.cn

Citation:
Yao, Y., Tian, Y., Andrews, C., Li, X., Zheng, Y., & Zheng, C. (2018). Role of groundwater in the dryland ecohydrological system: A case study of the Heihe River Basin. *Journal of Geophysical Research: Atmospheres*, *123*, 6760–6776. https://doi.org/10.1029/2018JD028432

Received 30 JAN 2018
Accepted 15 JUN 2018
Accepted article online 25 JUN 2018
Published online 7 JUL 2018

1. Introduction

Groundwater is critical for regulating the hydrological cycle and ecosystem water budget components in the natural system and sustaining the food production and drinking water needs for humans. Interpreting the role of groundwater in the ecohydrological systems will increase our understanding of the terrestrial water cycle and will also fill the knowledge gap of how climate changes, as identified in the fourth Intergovernmental Panel on Climate Change report, will impact ecohydrological systems (Change, 2007). However, it is extremely difficult to quantify the role of groundwater in a large-scale ecohydrological system. The first challenge is the discrepancy among various-scale data sets and models; typical groundwater models focus on aquifers, while the community ecology focus is mainly on a local scale (Griebler et al., 2014). The second challenge is how to separate the contribution of groundwater from confounding processes, such as quantifying the groundwater discharge to streams (Yao et al., 2015) and separating the contribution of groundwater from other sources to the evapotranspiration (ET) flux (Karimov et al., 2014). This study focuses on a dryland ecological system. In a typical dryland ecosystem, there is an upland mountainous area that provides a major source of water for downstream area through streamflow and mountain block recharge (MBR), a middle section with oases in which agricultural irrigation centers and stream and groundwater closely interacts, and a lower stream section in which streamflow is the only source of water for maintaining fragmented desert vegetation.

The functions of groundwater in the hydrological cycle include storing the meteoric inflow from precipitation, organizing the soil moisture and buffering climate fluctuations, partitioning the surface flow and lateral groundwater in the mountainous sources areas, and regulating the exchange flux with streams in the oasis plain with shallow water table (Miguez-Macho & Fan, 2012a, 2012b; Pokhrel et al., 2013). In terms of groundwater recharge (GWR), which refers to the net infiltration reaching to the aquifers, studies show that the ratio

between recharge and precipitation (i.e., also called infiltration factor) varies over a large range between 0.03 to 0.42 in arid and semiarid mountainous basins (Ball et al., 2014). Under long-term average precipitation conditions, this ratio is estimated to range between 0.001 and 0.005 across a large dryland (Scanlon et al., 2006). The GWR in irrigated areas is about 5 to100 times as much as in natural areas (Scanlon et al., 2005). This indicates that GWR is regulated not only by terrain but also by climate variability in time scale and land use/cover in spatial scale (Scanlon et al., 2006; Taylor et al., 2012). As opposed to the direction of water movement from precipitation to water table during the wet seasons, an upward groundwater flux for ET sustains vegetation in the dry season (Miguez-Macho & Fan, 2012b). Studies have estimated that about 10% of the water evapotranspired is directly contributed by groundwater, and this value can be up to 20–30% during the dry seasons (Lam et al., 2011; Yeh & Famiglietti, 2009). For drylands with high ratio of ET to precipitation, there is a need to evaluate groundwater's spatiotemporal contribution to ET.

Groundwater systems regulate the partitioning between baseflow and MBR in the upper-stream mountainous area and control the interaction with surface water in the alluvial plains. About 5% to 35% of recharge becomes MBR (Gleeson & Manning, 2008; Wilson & Guan, 2004; Yao, Zheng, Andrews, et al., 2017), which influences the hydrological processes of downstream alluvial plain by directly regulating streamflow and the level of the groundwater table. This regulation influences the other indirect hydrological processes such as ET, stream leakage, and groundwater discharge to surface water. Nevertheless, the extent to which upper-stream mountainous groundwater affects the middle and lower alluvial plain remains unclear. Meanwhile, since the groundwater system of the alluvial plain is closely linked with the stream network, they interact with each other through two-way exchange fluxes that vary seasonally (Miguez-Macho & Fan, 2012a). Even though advanced field experiments, such as distributed temperature sensing (Yao et al., 2015) and infrared remote sensing (Liu et al., 2016), provide insights for quantifying spatiotemporal interaction, the seasonal variability and hydrological pathways are not well understood in drylands.

Groundwater sustains ecosystems of drylands, which are very susceptible to change if water budget components are altered, directly by providing a source of water for vegetative uptake and subsequent ET. Indirectly, groundwater systems also buffer the precipitation and streamflow to maintain soil moisture for ET (Koirala et al., 2017; Tamea et al., 2009; Yao, Zheng, Tian, et al., 2017). Even though a groundwater-dependent ecosystem (GDE) is defined as a "natural ecosystem that requires access to groundwater to meet all or some of their water requirement on a permanent or intermittent basis, so as to maintain their communities of plants and ecosystem services" (Richardson et al., 2011), it is not easy to identify the relationship between groundwater and vegetation and map the GDE zones because the groundwater-vegetation interactions on large scales are difficult to quantify, particularly in desert plain with sparse vegetation. There are two major approaches for identifying the dependency of vegetation on groundwater. One approach is to employ an ecohydrological model. This type of model couples plant growth with the dynamic water movement between groundwater and the plant's roots, to quantify the groundwater dependence of a specific type of plant (Chui et al., 2011; Li, Zheng, et al., 2017). However, large-scale GDE zones are difficult to map by applying these ecohydrological models. Remote sensing products, such as leaf area index, normalized difference vegetation index, and gross primary productivity, are suitable to map GDE zones over a large scale (Doody et al., 2017; Koirala et al., 2017; Pérez Hoyos et al., 2016). Nevertheless, reliable diagnostic criteria must be designed for identifying the groundwater-vegetation interactions, which accommodate for the difference in time between the phenological (e.g., season of growth) and hydrological maximum (e.g., seasonal variation in the level of the water table or streamflow).

Therefore, we focus on the four following scientific gaps in this study: (1) the extent to which groundwater responds to precipitation and contributes to ET, (2) how groundwater system in the upper basin mountainous area influences hydrological processes in the downstream alluvial plain, (3) how groundwater regulates seasonal and annual cycle in streamflow, and (4) to what relevance and extent does groundwater sustains the vegetated ecosystem. We use the Heihe River Basin (HRB), the second largest endorheic river basin in China, as a typical basin in which to explore the role of groundwater in an ecohydrological system. As a water conflict exists between the middle stream agricultural system and the lower stream desert system, an integrated research strategy of water-ecosystem-economy was proposed and related studies on observations and modelings were conducted in the HRB (Cheng et al., 2014). The multiscale data sets, which are observed based on a hierarchically nested sensor network, were obtained to support deepening the understanding for complex eco-hydrological processes (Li, Liu, et al., 2017). The critical components in the water budget on the basin-

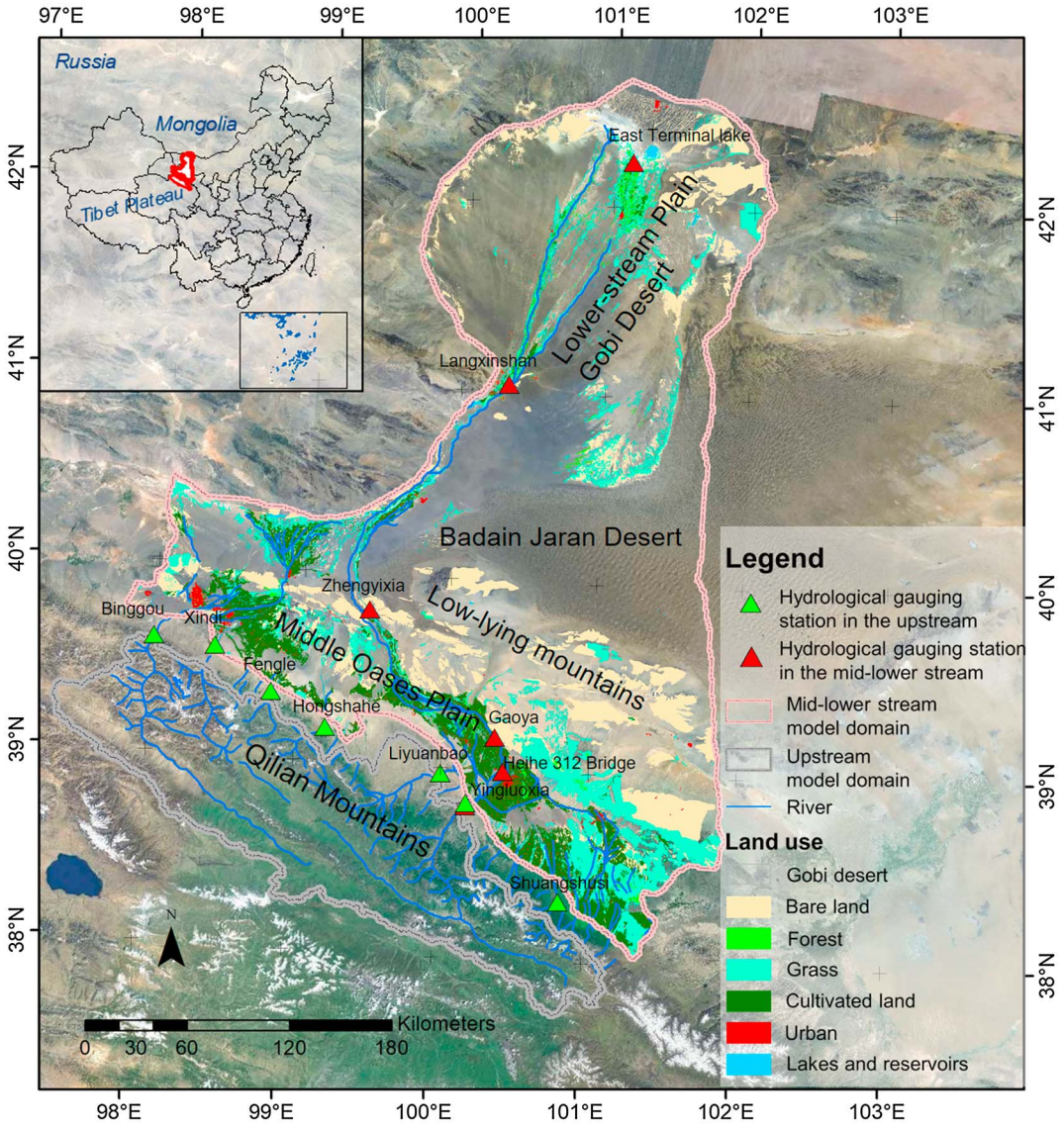

Figure 1. Study area: Heihe River Basin.

scale, along river segments and vertical irrigation system, have been quantified, respectively, by intervalidation between observed multiple data sets and model simulations (Li, Cheng, Ge, et al., 2018; Tian, Zheng, Zheng et al., 2015). These improvements provide an excellent research basis for unveiling the mechanism in our questions within the subsurface groundwater system. To address the scientific gaps, a well-calibrated regional-scale integrated model was employed to derive the spatiotemporal hydrological variables including water table depth, GWR, ET, and exchange flow with streams. A mountainous groundwater model was combined to test the sensitivity of hydrological variables of the mid-lower alluvial plain to the upstream mountainous groundwater system. Multiple independent databases of remote sensing products were used to identify correlation between groundwater and vegetation. The results of this study provide new general insights for water management of drylands globally.

2. Methodology

2.1. Background of Study Area

The HRB is located in the northwestern China, with a range between 97°E–102°E and 37°N–43°N (Figure 1). The basin stretches from the Qilian Mountains at the northern margin of the Tibetan Plateau, across the

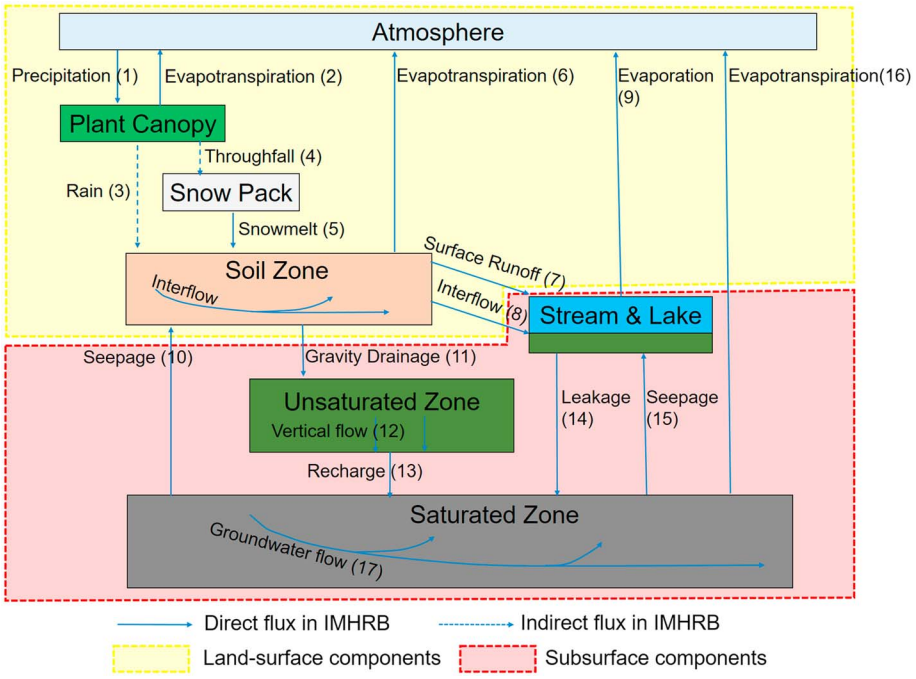

Figure 2. Schematic diagram of IMHRB.

middle stream oases, to terminal lakes in the Gobi desert just south of the Mongolian border. The elevation varies from over 5,600 m above mean sea level in the upstream mountains to less 900 m around the lower stream terminal lakes, covering a total area of about 143×10^3 km^2. The Gobi desert and mountainous terrain occupies about 58% and 33% of the total area, respectively, while the oases occupy less than 9% (Yao, Zheng, Liu, et al., 2014). The annual precipitation is up to 750 mm in the upstream mountainous areas but decreases to less than 50 mm in the lower desert plain (R. Ding et al., 2009). High ET with a rate over 500 mm/year occurs in the oasis areas along the streams, while the ET rate is between 20 and 100 mm/year in the Gobi desert areas (Tian, Zheng, Zheng, et al., 2015). The rivers originating in the Qilian Mountains are the main water resources maintaining the agriculture of the middle oasis plain and the fragile ecosystem of the lower stream desert plain.

The HRB consists of two major groundwater systems: upstream mountainous and mid-lower stream groundwater systems. A hydrological and ecological integrated watershed-scale model (referred to as IMHRB) was developed for the mid-lower stream groundwater system, with a model domain of 90,589 km^3, to simulate dynamic ecohydrological processes and evaluate regional-scale water budget (Tian, Zheng, Zheng, et al., 2015; Yao, Zheng, Liu, et al., 2014). Since the baseflow and MBR from the Qilian Mountains are the main sources of water inflow to the mid-lower alluvial plain, a 3-D numerical model of the mountainous groundwater system (i.e., hereinafter referred as QMGM), with a model domain of 23,728 km^3, was developed to quantify the partitioning between baseflow and MBR (Yao, Zheng, Andrews, et al., 2017).

2.2. Structure of Integrated Model

The hydrological and ecological integrated model of mid-lower stream plain (IMHRB) was developed based on GSFLOW (coupled groundwater and surface water flow model; Markstrom et al., 2008). The schematic diagram of IMHRB is shown on Figure 2. The IMHRB includes five fundamental hydrological components, which couple land-surface flow processes (bounded by yellow region on Figure 2) and subsurface flow processes (red region on Figure 2): atmosphere, soil zone, streams and lakes, unsaturated zone, and groundwater system. Simulation of land-surface flow focuses on evaluating the effects of climate and land use condition on water flows from atmosphere to soil zone, which consists of soil water relations, streamflow regimes, and GWR based on the PRMS (precipitation-runoff modeling system) model (Markstrom et al., 2015). The atmospheric component represents all climate drivers including precipitation, air temperature, and solar

radiation, all of which are used to compute infiltration, and ET. Precipitation intercepted by the plant canopy is considered, and the nonintercepted part is also regarded as part of snowpack, which is then infiltrated to soil zone when snow melting or accumulation depending on water-energy calculation. In this model, the soil zone is conceptualized as extending from the land surface to the base of the average rooting depth of the dominant vegetative type covering the soil surface, while the unsaturated zone extends from bottom of the soil zone to the saturated zone. The flow in the soil zone is determined by different water content thresholds (i.e., wilting threshold, field-capacity threshold, and preferential-flow threshold). The soil zone connects with streams and lakes via surface runoff and interflow.

Simulation of subsurface flow processes are used to characterize the vertical flow in the unsaturated zone, and the 3-D steady or transient flow in the aquifer system and flow to and from streams and lakes. Groundwater flow is simulated with MODFLOW-2005 (Harbaugh, 2005). The groundwater-regulated hydrological processes in this coupled model include (1) calculating recharge from precipitation to the saturated zone through soil and unsaturated zone using water-energy balance and kinematic wave method; (2) routing of surface water flows in a stream network through setting properties of stream channel and streambed, and calculating dynamic two-way exchange flux between aquifers and streams and lakes using water budget and Manning's equation; (3) calculating discharge from saturated to soil zone, which regulates the soil moisture and affects the ET of soil zone, and routing groundwater discharge to streams; and (4) calculating direct ET from saturated zone to atmosphere. The ET flux from the subsurface is simulated with the PRMS Soil Zone Module. However, where soils are thin and the root depth extends beneath the soil-zone base, ET is not satisfied by storage in the soil zone. In such a case, ET flux occurs from the unsaturated zone and the saturated zone, and the ET deficit is used to calculate transpiration from the unsaturated and saturated zones. The groundwater-related functions of IMHRB, which we briefly highlight here, are employed to investigate the role of unsaturated zone and the aquifer in the hydrological processes.

IMHRB has uniform regular grids for both the surface and subsurface domain and uses daily meteorological data and water use data (i.e., diversion, pumping, and irrigation) as the main forcing functions. This enables the model to explicitly and flexibly simulate agricultural water use activities (i.e., surface water diversion, groundwater pumping, and irrigation). Multiple data sets were used to calibrate this model, including long time series of observed groundwater levels as well as streamflow and independent data set derived from remote sensing products including ET and leaf area index. More details about forcing data, model parameters, and calibrations can be found in related published references (Tian, Zheng, Wu, et al., 2015; Tian, Zheng, Zheng et al., 2015; Yao, Zheng, Liu, et al., 2014).

2.3. Sensitivity of Hydrological Variables

The Qilian Mountains groundwater model (QMGM) was calibrated using stream baseflow estimates, which were computed from observed streamflow at seven hydrological gauging stations of upstream outlets (Yao, Zheng, Andrews, et al., 2017). To explore the extent to which the partitioning of recharge in the upper mountainous areas between baseflow and MBR affects hydrological processes in the mid-lower-stream plain, we linked QMGM with IMHRB. The baseflow and MBR from the Qilian Mountains, the upper portion of the HRB, were computed by the QMGM under a series of scenarios that resulted in various partitions of recharge between baseflow and MBR. The simulated MBR based on QMGM is the lateral groundwater inflow directly assigned to the flow boundary of IMHRB. The simulated baseflow from QMGM was added to the first segment downstream from the mountains where the Heihe flows into the mid-stream alluvial plain. The annually averaged partition (i.e., baseflow and MBR account for 65% and 35% of GWR, respectively) was defined as the baseline condition. The calculated hydrological variables include total ET (i.e., the actual evapotranspirated flux we used in this study), surface seepage from groundwater, stream leakage to groundwater (SLG), groundwater seepage to stream (GSS), and lake leakage to groundwater.

GWR and depth-dependent hydraulic conductivity (K) determine the absolute volume and relative partitioning between baseflow and MBR (Yao, Zheng, Andrews, et al., 2017). The depth-dependent hydraulic conductivity is represented by a general exponential decay model (Gleeson & Manning, 2008; Jiang et al., 2009; Yao, Zheng, Andrews, et al., 2017):

$$\log K_z = \log K_0 - Az \quad (1)$$

where K_z (m/s) and K_0 are the K at depth of z (m) and at the groundwater surface, respectively, and A is the decay exponent (m^{-1}).

The ratio between recharge and precipitation (GWR/P) and the decay exponent (A) of vertical hydraulic conductivity were used as a driver to detect the response of hydrological variables in the mid-lower plain. Under baseline condition, we increased GWR/P and A by 0.1 and 0.01, respectively, in the QMGM to calculate the corresponding change in baseflow and MBR, and linked the response to IMHRB. The response of each hydrological process was identified through a comparison between the baseline and changed model results. An elasticity index (EI), a dimensionless expression of sensitivity, was applied in this study to evaluate the relative change among hydrological variables with different orders of magnitude (Loucks et al., 2005; Yao, Zheng, Andrews, et al., 2017).

2.4. Identification of Groundwater-Vegetation Relationship

The depth to the water table (hereafter using DWT as groundwater table depth) determines if groundwater is a source of water to vegetation during the growing season. Therefore, a direct correlation relationship between DWT and net primary productivity (NPP) was evaluated for each phenological season based on the method proposed by Koirala et al. (2017). The DWT, at 1 km spatial and daily temporal resolutions, was generated from IMHRB. The NPP data between 2000 and 2006, with 1 km spatial and 10-day temporal resolutions, were obtained from West Data Center (http://westdc.westgis.ac.cn/). The phenological stages were defined by the magnitude of NPP in each climatological season. The seasons are defined as December to February, March to May, June to August, and September to November (Koirala et al., 2017). Through the climatological seasonal mean NPP, the month with maximum NPP was identified as maximum stage (maximum productivity). Through the change in NPP within each season (i.e., the change in seasonal NPP is calculated as the end-month NPP minus start-month NPP), the season with maximum positive change in NPP was identified as the greening stage. The correlation coefficient (r) between DWT (X) and NPP (Y) during the identified green stage was calculated for each model grid for n pairs using the following formula:

$$r = \frac{\sum_{i=1}^{n} (X_i - \overline{X})(Y_i - \overline{Y})}{\sqrt{\sum_{i=1}^{n} (X_i - \overline{X})^2} \sqrt{\sum_{i=1}^{n} (Y_i - \overline{Y})^2}} \quad (2)$$

3. Results

3.1. Groundwater Recharge and Evapotranspiration

The simulated spatial pattern of GWR, variability of infiltration to the soil zone, and saturated zone for the natural and anthropogenic land use groups in the Heihe basin are shown on Figure 3. The natural land use group includes bareland, forested, Gobi Desert, and grasslands. The anthropogenic land use group includes cultivated and urban lands. The GWR represents the water infiltrating to the water table, and the soil infiltration (Soilin) represents the water infiltrating below the land surface. The sources of water consist of areal recharge from precipitation, irrigation return flow, and seepage from streams, lakes, and wetlands.

In the middle oasis plain, with major cultivated and urban areas, the annual averaged GWR ranges from 5 mm to over 600 mm. Across the area of low-lying mountains, which separates middle-stream and lower-stream plain, the GWR is less than 1 mm/year due to low precipitation. Within the Badain Jaran Desert, the scattered lakes recharge the underlying aquifers at a rate of 6–20 mm/year. The GWR in the lower-stream plain is mainly from stream leakage and irrigation in the cultivated areas with a range between 1 and 50 mm/year.

As shown on Figure 3b, there is significant spatial variability in the GWR in the forested, cultivated, and urban areas, whereas the GWR in the bareland and Gobi Desert is relatively uniform. The ratio between soil infiltration and precipitation (Soilin/P) indicates the water supply contribution of precipitation to soil zone, and the ratio of GWR and precipitation (GWR/P) indicates the water supply contribution of precipitation to the saturated zone. For the vast areas of bareland and Gobi Desert, about 87% of precipitation on average infiltrates to the soil zone, but less than 1% reaches the groundwater table. Mean infiltration in the forested areas

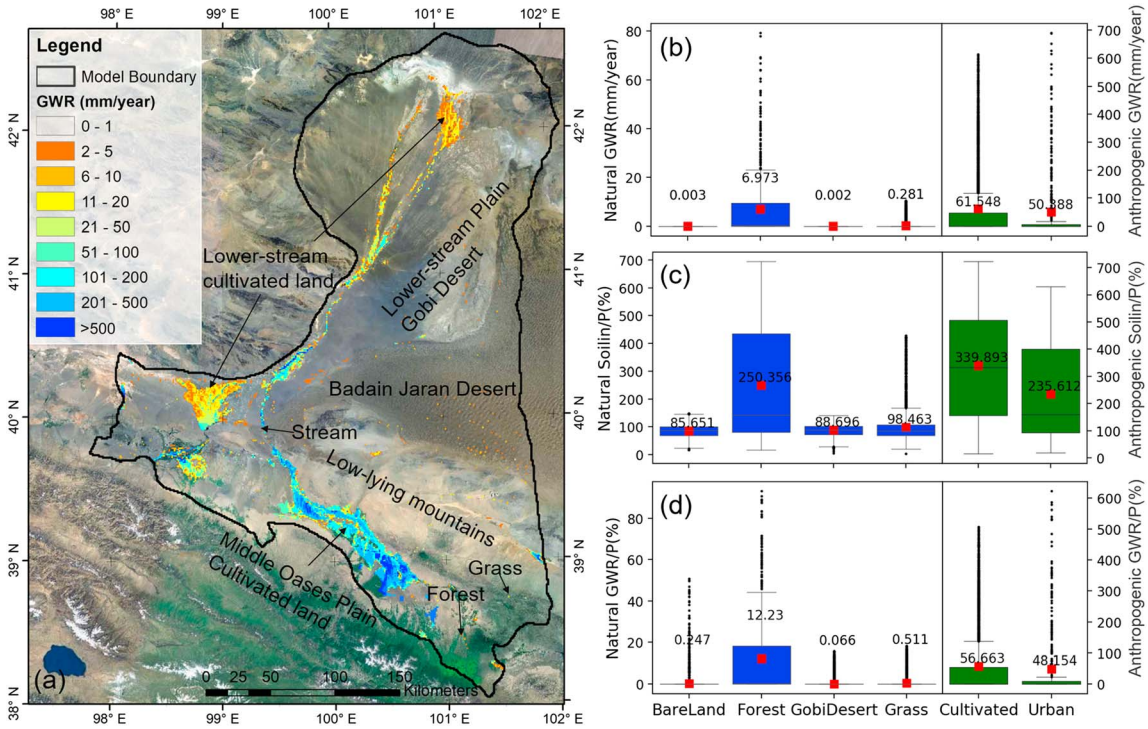

Figure 3. Distribution of (a) annual averaged GWR, variability (boxplot) of annual averaged (b) GWR, (c) Soilin/P, and (d) GWR/P under the natural (in blue) and anthropogenic land use types (in green), respectively. The transparent zone represents the area where the annual averaged GWR is below 1 mm/year. The red square in the boxplot represents the mean value of each data set marked with number above it.

exceeds precipitation by a factor of more than 2, and about 12% of precipitation reaches the groundwater table, which is significantly higher than that for other natural land use type. The high infiltration rate is the result of infiltration from the small tributaries in the forested areas that originate in the upper basin mountains. For cultivated lands, mean infiltration exceeds precipitation by more than a factor of 3 and over 56% of precipitation infiltrates to the water table due to infiltration of applied irrigation water. Infiltration from wetlands greatly contributes to the GWR in urban areas.

The distribution of the ET rate from groundwater (GWET), that is the flux directly evapotranspirated from the water table, and its variability under different land use types are presented in Figure 4. As shown in Figure 4a, the areas with GWET are located in the middle cultivated land, lower cultivated land, and alluvial plain edge with a broad range between 5 and 150 mm/year. In the areas where the groundwater is shallow (<1 m deep) or where the water table intersects streams and lakes, the GWET is over 300 mm/year. The averaged GWR represents high variability among different land use types, while the averaged GWET for five land use types keeps the same magnitude (below 10 mm/year) except for forest (Figure 4b). However, the total actual ET (AET) (i.e., the actual total evapotranspirated flux from both land-surface and subsurface part) extracted from simulated results shows that the land use greatly affects AET. This is reflected in the observation that the averaged value of AET in the anthropogenic land use group is significantly greater than that in the natural group. For the same group, the AET in vegetated land (forest and grass lands) is greater than bare land. The contribution of groundwater to AET is represented using a ratio between GWET and AET as shown in Figure 4d. Except for the forest land where groundwater contributes 8.7% on average to AET, the percentage in other land use types is below 3%, but for all there is a high variability in the ratio between GWET and AET.

The pattern of annually averaged depth to groundwater table (DWT) in the HRB is shown on Figure 5a. The areas where groundwater is shallower than 2 m cover about 11% of the middle and lower plain. A shallow water table exists mainly along the streams and the edges of the alluvial plain. The areas in which DWT is less than 10 m account for 41% of total model domain. The groundwater table is over 100 m deep, which accounts for 27% of total model areas, in much of the low-lying mountainous and desert areas.

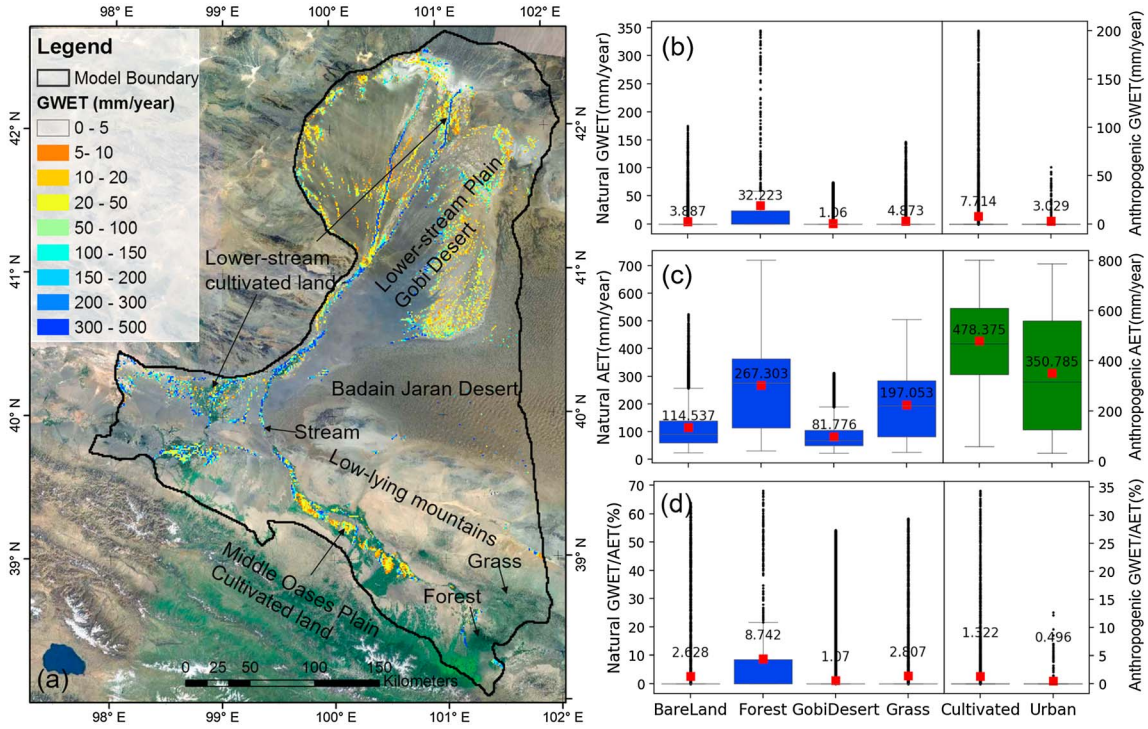

Figure 4. Distribution of (a) annual averaged GWET, variability (boxplot) of annual averaged (b) GWET, (c) AET, and (d) ratio of GWET/AET under the natural (in blue) and anthropogenic (in green) land use group, respectively. The red square in the boxplot represents the mean value of each data set marked with mean value posted above it.

The middle and lower alluvial plain has four subbasins: Zhangye and Jiuquan in the middle alluvial plain and Jinta and Ejina in the lower alluvial plain. These subbasins are defined by geological structures (Yao, Zheng, Tian, et al., 2014). Since the climate regime, topography, and geological setting are much differences between the middle and lower plain, we analyzed the annual and seasonal DWT, GWR, and GWET in the Zhangye and Ejina basins, respectively, to illustrate the differences. In the Zhangye subbasin, where averaged DWT is less 2 m (Figure 5b), the maximum annual mean GWR was over 500 mm in 2010. The peak GWR occurs in August with a mean monthly GWR of over 50 mm. The annual maximum mean GWET was about 67 mm in 2005 with a peak mean monthly GWET in June of 9 mm. The highest water table elevations occur in March and the minimum water table elevations occur in July.

In the areas of Zhangye subbasin where DWT ranges between 2 and 5 m (Figure 5c), the annual and seasonal patterns of GWR are similar to that in areas where depth to water table is less than 2 m but magnitude of GWR is much smaller: 164 mm/year and 17 mm/month for maximum annual and seasonal, respectively. The annual pattern of GWET for the areas with DWT between 2 and 5 m is different from the areas with DWT less than 2 m (Figure 5b), reflecting that the maximum annual GWET changes to the year of 2011 with a value of 32 mm/year. The seasonal cycle is similar to Figure 5b in which the peak season occurs at June but the maximum monthly GWET is only 3.4 mm. The annual variation of DWT in areas with depth between 2 and 5 m is between 3.7 and 3.4 m, and seasonal variation is between 3.5 and 3.4 m (Figure 5c).

For the area with averaged DWT between 5 and 10 m, the maximum annual and monthly GWET is 5.3 and 0.57 mm, respectively (Figure 5d). The seasonal pattern of GWET is similar to that shown on Figure 5c. Even though the GWR and GWET are small in these areas, the annual and seasonal variations of DWT are about 0.7 and 0.27 m, respectively.

The annual and seasonal GWR, GWET, and DWT in the lower Ejina subbasin were plotted for different groundwater depths. For the area where annually averaged DWT is less than 2 m, the maximum annual GWR was about 5.4 mm in 2003 and the seasonal variation was between 0.57 mm/month in October and 0.02 mm/month in June, while the maximum annual GWET is about 68 mm and the seasonal variation is between

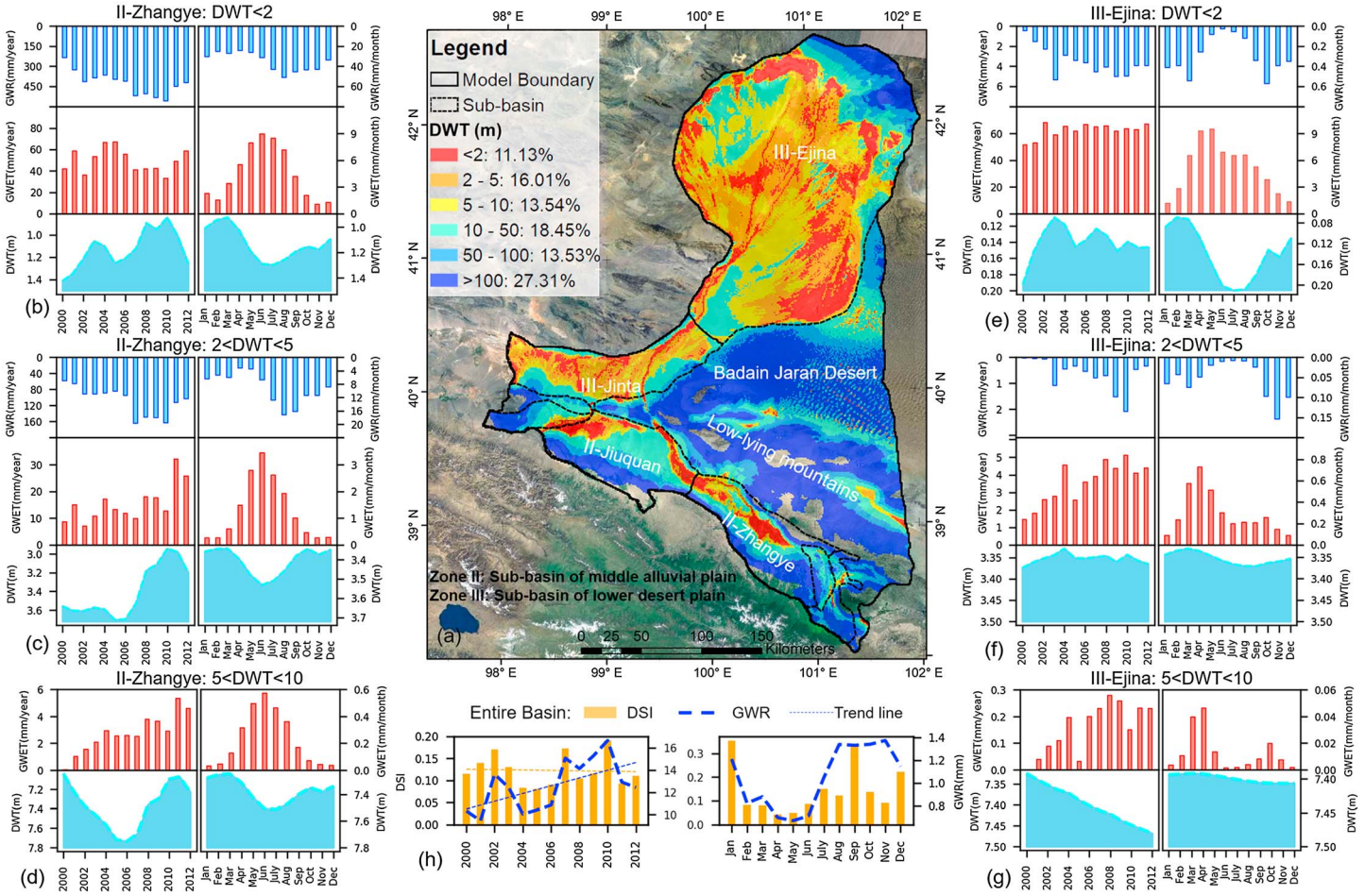

Figure 5. (a) Distribution of annually averaged DWT. Annual variability and seasonal cycle of GWR, GWET, and DWT for subbasin of (b–d) Zhangye and (e–g) Ejina under different DWT conditions, respectively. (h) Annual and seasonal averaged DSI and GWR for the entire basin.

9.5 mm/month in May and 1.2 mm/month in January (Figure 5e). The annual variation of DWT in this area is between 0.1 and 0.2 m, and seasonal variation of DWT is between 0.07 in March and 0.21 m in July.

For the areas in which the averaged DWT is between 2 and 5 m (plotted on Figure 5f), the maximum annual GWR was 2.1 mm in 2010 and seasonal variation varied between 0.15 mm/month in November and 0.007 in July. Compared with the areas where DWT is less than 2 m, the maximum annual GWET is almost tenfold smaller with a value of 5.1 mm/year (in 2010) and the seasonal variation of GWET is between 0.72 mm/month in April and 0.08 mm/month in December. The annual variation of DWT in this area is between 3.37 and 3.32 m, and the seasonal variation of DWT is between 3.33 m in March and 3.37 m in September. For the area with an averaged DWT over 5 but less than 10 m, the GWR is very small, and the mean annual GWET is about 0.28 mm and seasonal variation of the GWET varies only between 0.05 and 0.002 mm/month in April and December, respectively. The mean annual DWT ranged from 7.46 to 7.32 m during the period 2000 to 2012, and the mean seasonal DWT was relatively stable varying between 7.41 and 7.39 m.

The climate regimes are represented by the ratio of annual averaged precipitation to potential ET (Scanlon et al., 2006). This ratio is known as the drought severity index (DSI). Figure 5h plots the annual and seasonal DSI and GWR for the entire middle and lower alluvial plain. During the model period between 2000 and 2010, the GWR had a significantly increasing trend, but the DSI does not exhibit a corresponding trend. During the modeled period, the most hyper-arid season occurred in April and the wettest season occurred in January.

3.2. Sensitivity of Hydrological Variables to Recharge in Mountainous Area

The sensitivity in volume and EI of each hydrological variable responding to the changing GWR/P and A of upper mountains is summarized on Table 1. A positive EI represents that when GWR/P or A increases

Table 1
Summary of Response in the Hydrological Variables of the Middle and Lower Alluvial Plain to the Groundwater Recharge Ratio (GWR/P) and Decay Exponent of Hydraulic Conductivity (A) of Upper Mountains

Factor		LGI	SLG	LLG	ET	SS	GSS	GSL
GWR/P ↑0.01	%	↑5.59	↑0.62	↓ −0.51	↑1.44	↑1.08	↑0.06	↑0.97
	EI	1.01	0.11	−0.09	0.26	0.19	0.01	0.17
A ↑0.001	%	↓ −11.23	↑0.73	↑0.34	↓ −1.98	↓ −0.17	↓ −0.49	↓ −1.96
	EI	−0.48	0.03	0.01	−0.08	−0.01	−0.02	−0.08

(decreases), the corresponding hydrological variable increase (decrease), while a negative EI represents the opposite case. Except for the LLG, other hydrological variables exhibit a positive response to GWR/R. However, except for the SLG and LLG, all others represent a negative response to A.

The major hydrological processes in the entire HRB and the hydrological connections between mountainous groundwater system and the downstream alluvial plain are shown on Figure 6. As the groundwater flow from the mountain block (MBR), the LGI is the most sensitive variable to the GWR and depth-dependent K of the upper mountains (i.e., the volume of LGI increases about 5.6% of original LGI). ET is the second sensitive variable with a 1.44% increasing when GWR/P increasing. It indicates the GWR subject to climate regimes of the upper mountains would have an indirect positive effect on the hydro-ecological system of the mid-lower alluvial plain. Two-way exchange flux including stream-groundwater and lake-groundwater are also influenced but with a relatively moderate magnitude.

3.3. Contribution of Groundwater to Streamflow

The spatial pattern of the annual flux of groundwater from/to the five major stream segments in the upper and lower HRB, in mm/year, is represented in Figure 7a. These five segments are defined by six hydrological gauging stations. The annual amount of SLG along the main stream of Heihe ranges from 100 to 500 mm, while the annual amount of GSS, centered in the segment between Heihe 312 Bridge and Zhengyixia, varies between −200 and −600 mm/year. The annual amount of SLG along tributaries of the Heihe ranges from 0 to 100 mm/year.

There are three stream segments in the middle oasis plain from Yingluoxia to the Zhengyixia station. The first segment is from the outlet of Qilian Mountains (Zhengyixia) to Heihe 312 Bridge where stream leakage is the main source of recharge to the groundwater. Surface runoff (Qs) contributes about 37% of streamflow in this segment, and 27% of streamflow on average recharges the groundwater (Qg) through the thick unsaturated

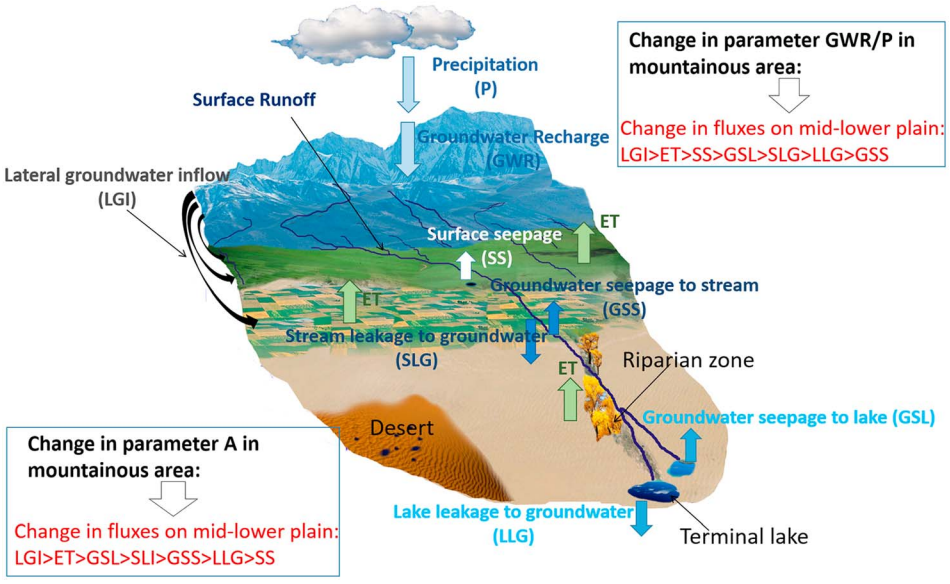

Figure 6. The conceptual diagram of hydrological processes in an arid river basin, highlighting the response of mid-lower hydro-ecosystem subject to upstream mountainous groundwater system.

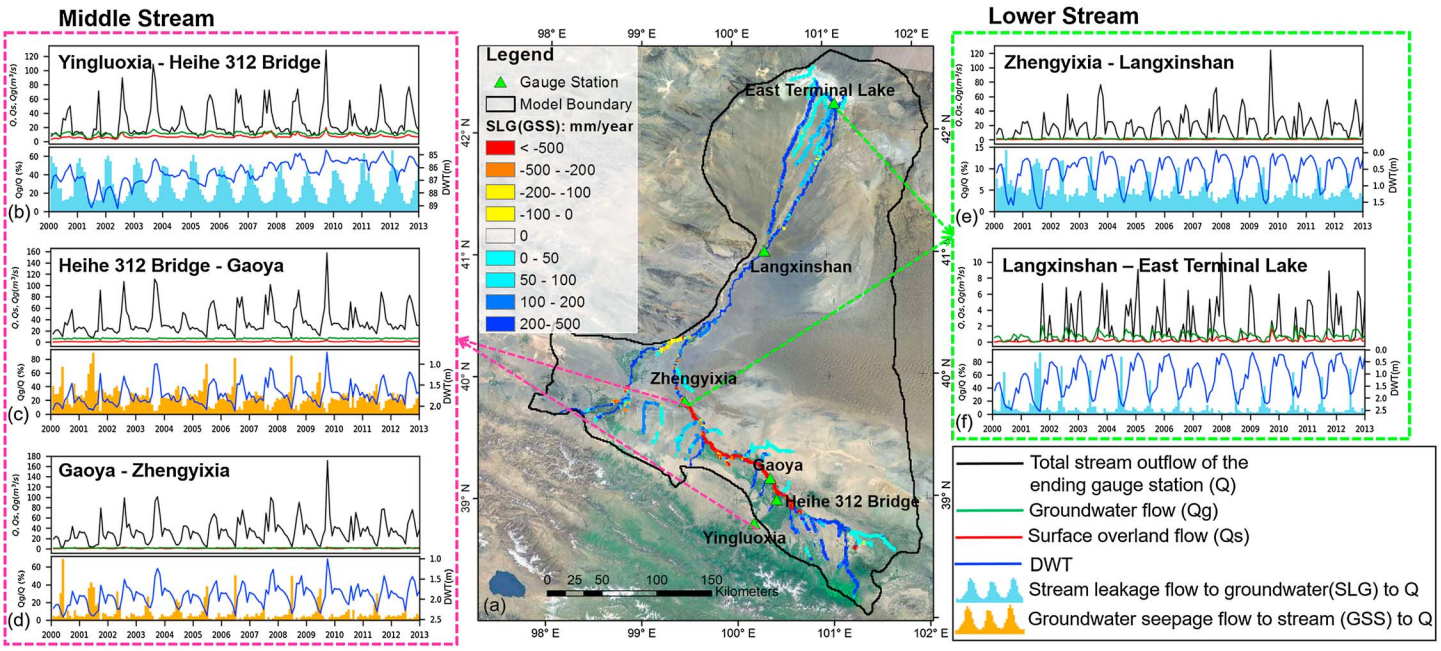

Figure 7. Spatiotemporal distribution of groundwater-surface water interaction. (a) A positive value of SLG and a negative value of GSS represent the spatial flow of stream leakage to aquifers and groundwater seepage to the stream in a spatial distribution, respectively. Variations in monthly streamflow (Q), the absolute value of SLG and GSS (Qg) and surface runoff (Qs), mean groundwater table depth (DWT), and fraction of groundwater contribution to total streamflow (Qg/Q) along middle stream segment of (b) Yingluoxia and Heihe 312 Bridge, (c) Heihe 312 Bridge and Gaoya, and (d) Gaoya and Zhengyixia, along lower stream segment of (e) Zhengyixia and Langxinshan and (f) Langxinshan and Eastern terminal lake.

zone where DWT is over 80 m deep (Figure 7b). The seasonal variation of the leakage flux is between 3.8 and 17.0 m^3/s occurring in September and March, respectively, while seasonal groundwater contribution (Qg/Q) is between 26% and 55% occurring in July and January, respectively. The seasonal DWT varies within a range of 1.5 m, from a depth of 86.9 m in May to 85.6 m deep in October, indicating an approximate one-month lag in the water table response to streamflow infiltration.

The second segment is from Heihe 312 Bridge to the gauging station Gaoya. In this segment, groundwater seepage dominates the two-way exchange with a relatively shallow groundwater depth of about 2 m. As shown in Figure 7c, the groundwater seepage and surface runoff contribute 25% and 3% of streamflow on average, respectively. The seasonal variation of Qg is between 5.2 m^3/s in September and 7.5 m^3/s in October, while the groundwater contribution is as much as 60% of streamflow in June and as little as 7% of streamflow in September. The seasonal DWT ranges from 1.8 m deep in June to 1.3 m deep in September.

The third segment is from Gaoya to the gauging station of Zhengyixia. In this segment, the groundwater seepage also dominates the two-way exchange. As shown in Figure 7d, the Qg from GSS contributes 8% of streamflow while Qs only contributes 3.9% of the streamflow. The seasonal pattern of Qg is same as that in the upstream segment, but the maximum flux is only 2.0 m^3/s in October and minimum flux is 0.55 m^3/s in September. The contribution of groundwater is less than that in upstream reach, as it is 24% in the peak season of June and less than 1% in September.

The Heihe enters the lower desert plain downstream through gauging station Zhengyixia. The first segment in the lower alluvial plain is from Zhengyixia to the gauging station Langxinshan. In this segment, stream leakage is the main source of GWR and DWT fluctuates in response to streamflow. Qg accounts for 5% of streamflow on average, and seasonal cycle ranges from low flux of 0.64 m^3/s in June to high flux of 2.25 m^3/s in September (Figure 7e). The average DWT varies from 1.2 m in June to 0.15 m in March due to high streamflow and low GWET in the winter.

The last segment is the eastern branch of main stream of the Heihe from Langxinshan to the gauging station East Terminal Lake. In this segment, SLG is also the main source of GWR even though streamflow significantly decreases downstream of Langxinshan. Qg accounts for 11% of total streamflow and up to 42% of

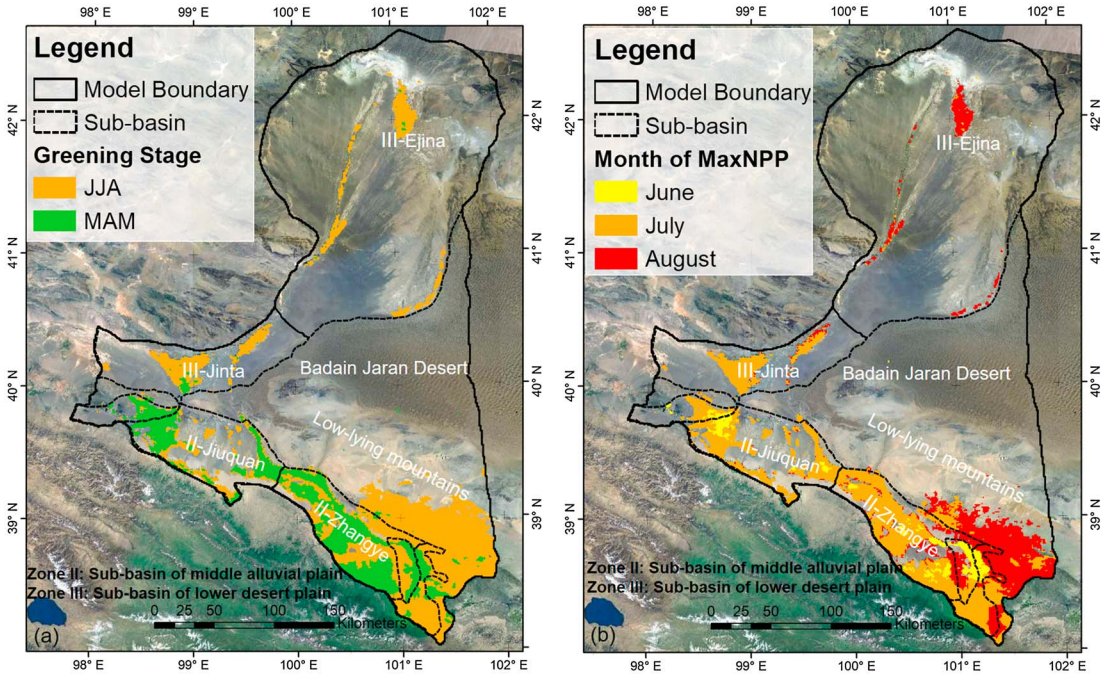

Figure 8. Spatial patterns of (a) the month of the greening stage and (b) the month with the maximum NPP values (MaxNPP). December to February (DJF), March to May (MAM), June to August (JJA), and September to November (SON).

streamflow in June, which is the lowest flow month (Figure 7f). The average seasonal DWT varies between a maximum of 2 m in June to a minimum of 0.7 m March.

3.4. Relationship Between Groundwater and Vegetation

Spatial patterns of the seasonal timing of greening stage and the month of maximum NPP values were identified with NPP data as shown on Figures 8a and 8b, respectively. There are two distinct seasonal patterns in the greening stage in the middle and lower alluvial plain. The pattern with the greening stage between June and August mostly is natural vegetation, covering 68% of the vegetated land, while the pattern with the greening stage between March and May mostly is cultivated land, which covers 32% of the vegetated land. The timing of the maximum stage varies from June and July on the cultivated lands to August on the lands with natural vegetation.

The correlation coefficient between NPP and DWT for each model grid covered with vegetation during greening and maximum stages are shown on Figure 9a. Positive relation (i.e., when the NPP is increasing and the DWT is increasing) accounts for about 78% of the calculated areas, while a negative relation (i.e., when NPP is increasing, the DWT is decreasing) accounts for 21% of the area. In the naturally vegetated area, which is centered in the Zhangye basin and low-lying mountains, over 73% of the area has a negative correlation with DWT. In the vegetated lower desert area, there is a positive correlation with DWT in over 80% of the area.

The fraction of AET from groundwater (GWET) was extracted as shown on Figure 9b. In the middle oases, the area in which the contribution of GWET over 10% only accounts for 3% of the area of the Zhangye Basin. However, in the lower desert plain, the GWET/AET greater than 10% accounts for 13% of the area of the Ejina Basin, and GWET/AET over 50% accounts for about 6% of the area of the Ejina Basin. The fraction of GWET in AET indicates the amount of the direct contribution of groundwater to NPP and ecosystem health.

4. Discussion

4.1. Groundwater Responses to Land Surface Regime

The results of model simulations based on IMHRB quantify the spatiotemporal characteristics groundwater system response to land surface regime, which includes the climate state (i.e., precipitation and

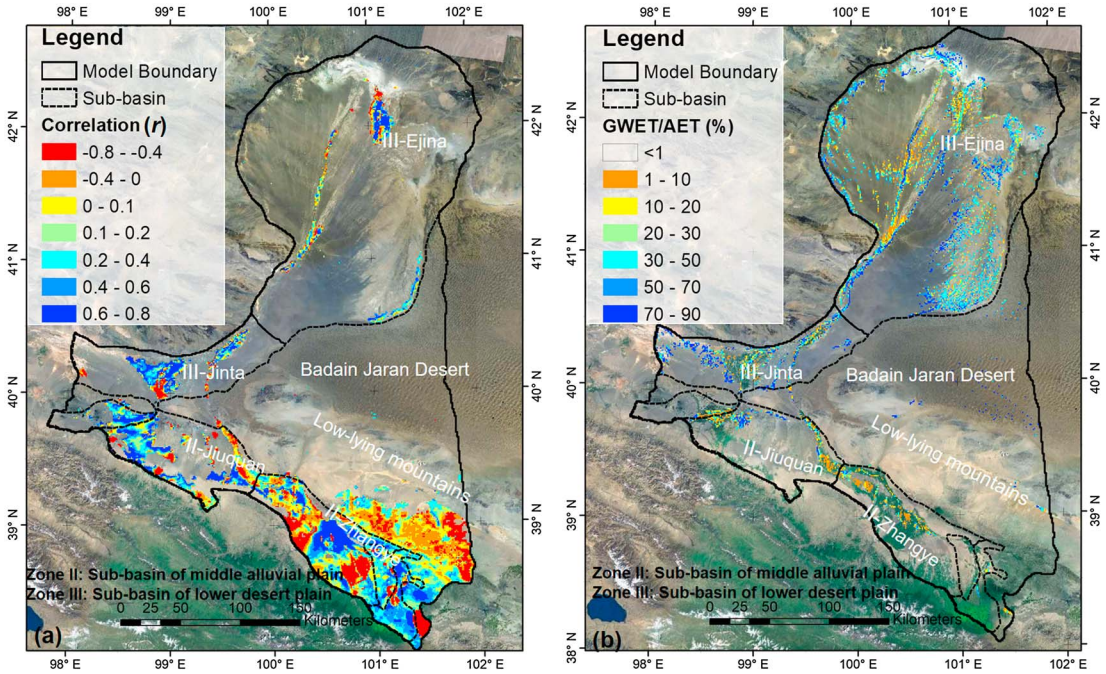

Figure 9. Distribution of (a) NPP-DWT correlation and (b) groundwater contribution to AET (GWET/AET).

temperature) and human activities (i.e., land use and irrigation). GWR within the modeled domain varies widely from approximately 0 mm/year in the Gobi Desert to over 600 mm/year in cultivated areas. GWR in the forested, cultivated, and urban areas has significant variability, ranging over 2 orders of magnitude, indicating that local specific factors need to be considered in anthropogenic areas when estimating GWR. In nonvegetated areas, GWR is relatively uniform, though the ratio GWR/P is variable. Our results of land use-determined recharge is consistent with other relevant studies (Qin et al., 2011; Scanlon et al., 2006). These results suggest that climate change will not impact GWR significantly in nonvegetated areas, instead, the hydrologeogical settings determine the magnitude of the GWR. The annual GWET has a lower dependency on land use (i.e., mean annual GWET under all land use types, except for forested, ranges from 0 to 7.7 mm/year), even though the total AET is greatly influenced by land use. However, the GWET represents a higher variability within land use type because of the difference in DWT. Annual and seasonal analyses for middle and lower alluvial plain (Figure 4) indicate that both GWR and GWET are depth-dependent variables that are constrained by land surface regime.

GWR and GWET coimpact the dynamics of DWT and water budget of groundwater systems. As indicated by our results, the groundwater budget differs substantially between the middle oasis plain and the lower deserted plain, and between shallow and deep aquifers. On the one hand, in the middle oasis plain (Zhangye Basin) recharge (e.g., over 400 mm/year) is much greater than GWET (e.g., below 100 mm/year), whereas in the lower desert plain (Ejina Basin) recharge (e.g., less than 6 mm/year) is much less than GWET (e.g., over 60 mm/year) where DWT is less than 2 m. On the other hand, the imbalance, manifested in the sufficient GWR for shallow aquifers and the scarce recharge for deep saturated aquifers, reveals the risk of exhaustion of deep aquifers. The drought by climate change (e.g., decreasing precipitation and rising temperature) and human activities (e.g., pumping water from deep aquifers) would further exacerbate this imbalance.

4.2. Mountainous Groundwater System Regulates Hydrological Processes of Downstream Alluvial Plain

The results from sensitivity simulation with QMGM linked to IMHRB quantify the extent to which the groundwater system in the upper mountains regulates the hydrological process in the downstream alluvial plain. The lateral flow from MBR directly recharges the aquifers of the middle basins. The MBR plays an important role in sustaining the thick aquifers of piedmont in the middle alluvial plain. Meanwhile, MBR has a great

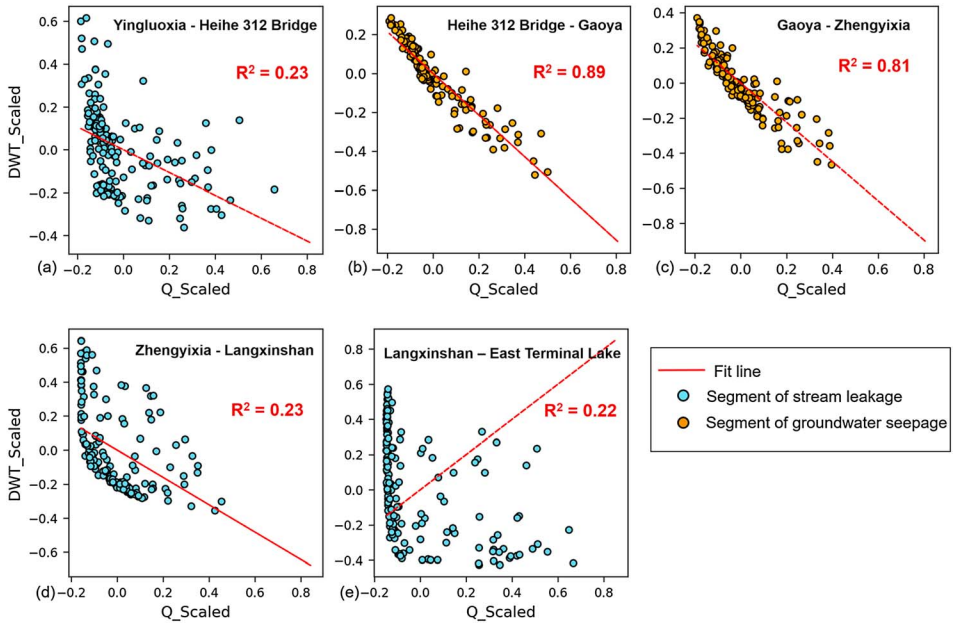

Figure 10. Correlation between streamflow (Q) and negative DWT for each segment of middle and lower streams. The Q and negative DWT were normalized as DWT_Scaled and Q_Scaled, respectively.

impact on the dynamics of DWT for shallow groundwater, then the changing DWT will affect the GWR and AET. Furthermore, the results indicate that the partition between baseflow and MBR, controlled by mountainous groundwater, regulates streamflow and stage and the elevation of the water table. This regulation impacts the two-way exchange between the groundwater system and the stream system.

Baseflow and MBR from the mountainous groundwater system are substantial water resources for the middle alluvial plain. The effects of climate change on mountainous areas can be amplified in the hydrological processes of the downstream alluvial plain. The uncertainty of the GWR of upper mountains can lead to a biased estimate for the mid-lower plain. Meanwhile, the depth-dependent K in the mountain block has a relatively smaller impact on hydro-ecological processes based on a comparison of E value between GWR/P and A. Thus, reasonable assumptions on hydrogeological characteristics in data-limited upper mountains are appropriate when estimating the water budget on a regional scale.

4.3. Groundwater Regulates Streamflow

The simulated results from IMHRB help identify the extent to which groundwater regulates streamflow on the alluvial plain. Different average contributions of groundwater (Qg/Q), among the five stream segments that span the entire alluvial plain, ranging from 5% to 27%, indicate that processes of infiltration and seepage are constrained by the local hydrogeological settings including topography, geology, and land cover. The five segments of the Heihe exhibit different exchange dynamics in magnitude but all indicate a wide range of seasonal variation in groundwater's contribution between the wet and dry seasons. In the segment between Yingluoxia and Heihe 312 Bridge, which has a thick unsaturated zone, stream leakage is greater than 50% of streamflow in the dry season and only about 10% of streamflow in the wet season, which means that the aquifers with high permeability in this piedmont area act as a natural "reservoir." Along the seepage segment of the middle stream (Heihe 312 Bridge-Gaoya), groundwater provides the bulk of streamflow in the dry season (over 60%), indicating that groundwater controls the dynamics of the stream in the dry season. Along the lower segment of the Heihe in the lower desert plain (Langxinshan-East Terminal Lake), over 95% of streamflow infiltrates to groundwater in extremely dry seasons, indicating that declining groundwater levels during dry periods exacerbate the processes of stream leakage. Our results supplement and improve our knowledge of seasonal variation of groundwater's contributions to streamflow compared to previous estimations (H. Ding et al., 2012; H. Ding et al., 2006; Zhao et al., 2011). There is a strong correlation between DWT and Q for the seepage segments, whereas no correlation for the leakage segments as represented (Figure 10).

The strong correlation in the seepage section can be explained by the support of groundwater to stream, and a synchronous change in both groundwater and streamflow is implicated in monthly resolution. Delayed response of groundwater to stream leakage in part explains the insignificant correlation for the leakage segments, and this delayed time of leakage process could be over one month. Lateral flow and GWET, which affect the groundwater system budget, are also the reasons for this insignificant correlation. These results indicate that using correlation between groundwater table and streamflow to evaluate leakage function will lead to a confusing result. Integrated modeling between groundwater and surface water is effective for characterizing the two-way exchange processes.

4.4. Groundwater-Sustaining Ecosystems

Spatial patterns of correlation between DWT and NPP illustrate the relationship between groundwater and vegetation. Strong positive correlation, increasing DWT (declining water table) with growing vegetation (increasing NPP values) occurred in the flat vegetated areas, is explained by groundwater contributing water for ET. Whereas, a strong negative correlation, decreasing DWT (rising water table) with growing vegetation occurred in the anthropogenic areas, is explained by increased surface recharge (e.g., irrigation from diverting stream or reservoir).

The pattern of groundwater's contribution to ET not only indicates the extent to which groundwater directly sustains the vegetation but also manifests its function in maintaining soil moisture of desert plain. As shown in Figure 9b, the ratio GWET/AET is greater than 70% in the southeastern areas of the Ejina subbasin, adjacent to the Badain Jaran Desert. It further implicates the critical role of shallow groundwater in preventing desertization but causing salinization of soils and creating conditions not conducive to vegetative growth. Moreover, although deep groundwater does not directly provide a source of water for vegetation, it serves as a "temporary bank" to retain the groundwater level on basin scale through lateral groundwater flow (Yao, Zheng, Tian, et al., 2017). The identification of the spatial extent of groundwater-dependent ecosystem must consider the entire groundwater system.

4.5. Implication for Water Management and Limitations

The historical analyses on groundwater's function in hydrological processes and ecosystem processes not only increase the knowledge on physical processes but also provide useful insights for water management and policy making for arid river basins globally. Since changes in the partition of baseflow and MBR will disturb all hydrological processes across the entire river basin, development of additional reservoirs should be carefully considered, for example, the proposed project of Huangzangsi Dam in the upper mountainous areas of HRB (Chen et al., 2005). The contrasting groundwater systems between middle and lower plain, illustrated by complex GWR and GWET patterns and stream dynamics, require different water management policies. For middle oasis plain, restrictions on pumping from deep aquifers are recommended, because the depletion of deep aquifers would cause the unrecovered damage. For lower oases, an adaptive regulation is suggested for environmental streamflow (i.e., regulating streamflow downstream of Zhengyixia to maintain lower desert ecosystem) rather than a fixed volume control (Li, Cheng, Ge, et al., 2018).

The hydro-ecological processes discussed in this study are based on model simulations and remote sensing products with monthly time resolution and 1 km spatial resolution. Potential biases exist from down scaling physical and anthropogenic parameters to a finer resolution (Li, Cheng, Lin, et al., 2018). For example, growing characteristics of scattered vegetation are poorly represented by NPP data with 1 km resolution. However, the results of this study provide the fundamental analyses for eco-hydrological research on a regional scale. This study has provided critical values and ranges for GWR and GWET, fractions for contribution of groundwater to ET and streamflow, and relationships between DWT and NPP.

5. Conclusions

A comprehensive analysis was made based on numerical simulations and data analyses to quantify groundwater characteristics in the arid eco-hydrological system of the HRB. Spatiotemporal patterns of recharge and groundwater contribution to ET were characterized based on the integrated model IMHRB developed for the middle and lower alluvial plain of HRB and the upstream mountainous groundwater model of QMGM. Effects of upper mountainous groundwater system on hydrological processes of the downstream alluvial plain were evaluated by linking QMGM with IMHRB. The influence of groundwater on streamflow dynamics were

quantified by analyzing the two-way exchange flux between groundwater and surface water along five segments of the Heihe. The relevance between groundwater table depth and vegetation was identified, and the extent to which the groundwater contributes to the vegetation was quantified by the simulated groundwater table and independent data sets of NPP. Major study findings include the following:

1. The area in which groundwater table is within 10 m of land surface covers over 40% of mid-lower alluvial plain. In this area, both recharge and ET of groundwater are dependent on water table depth, yet the recharge is more affected by land use than groundwater ET. In vegetated areas, the GWR has a higher variability with recharge rates ranging over 2 orders of magnitude. Seasonal variation in the water budget is dominated by recharge and ET of the shallow groundwater.
2. MBR acts as the primary source of lateral flow maintaining a stable groundwater system in the piedmont area. The partition between baseflow and MBR, which is controlled by upstream groundwater system, impacts the ET and two-way exchange between groundwater and surface water systems of the downstream alluvial plain.
3. Aquifers with a thick unsaturated zone in the piedmont area serve as "natural reservoir" storing water from stream leakage (over 50% of streamflow in the dry season and about 10% in the wet season). Groundwater dominates the streams by contributing about 40% streamflow in the dry season along the seepage segment middle alluvial basin, represented as groundwater table strongly positive correlating with streamflow.
4. Groundwater sustains ecosystem directly by providing water for ET in the growing season of vegetated areas with shallow groundwater table, as demonstrated by a strong positive correlation between groundwater table depth and NPP. Aquifers particular near streams also sustain ecosystem in an indirect way of buffering the stream leakage for aquifers far away from streams through lateral flow.

Our study concludes that development of additional reservoirs in the upper stream should be carefully considered. Our study also suggests restrictions on pumping from deep aquifers of the middle oasis plain and an adaptive regulation and design on streamflow and land use for lower desert plain, respectively. The findings in this study provide valuable knowledge for other regional studies in other dryland regions.

Acknowledgments
This work is supported by the National Natural Science Foundation of China (NSFC) research program "An integrated study of eco-hydrological processes in the Heihe River Basin, northwest China" (grants 91225301, 91425303, and 41501024) and by an additional NSFC research project (grants 41330632) and Shenzhen Municipal Science and Technology Innovation Committee (JCYJ20160530190547253). All data reported in this paper can be accessed in the cited references.

References

Ball, L. B., Caine, J. S., & Ge, S. (2014). Controls on groundwater flow in a semiarid folded and faulted intermountain basin. *Water Resources Research*, *50*, 6788–6809. https://doi.org/10.1002/2013WR014451

Change, I. C. (2007). The Fourth Assessment Report of the Intergovernmental Panel on Climate Change, *Geneva, Switzerland*.

Chen, Y., Zhang, D., Sun, Y., Liu, X., Wang, N., & Savenije, H. H. G. (2005). Water demand management: A case study of the Heihe River Basin in China. *Physics and Chemistry of the Earth, Parts A/B/C*, *30*(6–7), 408–419. https://doi.org/10.1016/j.pce.2005.06.019

Cheng, G., Li, X., Zhao, W., Xu, Z., Feng, Q., Xiao, S., & Xiao, H. (2014). Integrated study of the water-ecosystem-economy in the Heihe River Basin. *National Science Review*, *1*(3), 413–428. https://doi.org/10.1093/nsr/nwu017

Chui, T. F. M., Low, S. Y., & Liong, S.-Y. (2011). An ecohydrological model for studying groundwater–vegetation interactions in wetlands. *Journal of Hydrology*, *409*(1–2), 291–304. https://doi.org/10.1016/j.jhydrol.2011.08.039

Ding, H., Hu, X., Lan, Y., Shen, Y., Yin, Z., & Li, L. (2012). Characteristics and conversion of water resources in the Heihe River Basin. *Journal of Glaciology and Geocryology*, *34*(6), 1460–1469.

Ding, H., Zhang, J., Lu, Z., Yang, K.-y., Li, J., & Niu, X.-m. (2006). Characteristics and cycle conversion of water resources in the Hexi Corridor. *Arid Zone Research*, *2*(8), 241–248.

Ding, R., Wang, F.-c., Wang, J., & Liang, J.-n. (2009). Analysis on spatial-temporal characteristics of precipitation in Heihe River Basin and forecast evaluation in recent 47 years. *Journal of Desert Research*, *29*(2), 335–341.

Doody, T. M., Barron, O. V., Dowsley, K., Emelyanova, I., Fawcett, J., Overton, I. C., et al. (2017). Continental mapping of groundwater dependent ecosystems: A methodological framework to integrate diverse data and expert opinion. *Journal of Hydrology: Regional Studies*, *10*, 61–81. https://doi.org/10.1016/j.ejrh.2017.01.003

Gleeson, T., & Manning, A. H. (2008). Regional groundwater flow in mountainous terrain: Three-dimensional simulations of topographic and hydrogeologic controls. *Water Resources Research*, *44*, W10403. https://doi.org/10.1029/2008WR006848

Griebler, C., Malard, F., & Lefébure, T. (2014). Current developments in groundwater ecology—From biodiversity to ecosystem function and services. *Current Opinion in Biotechnology*, *27*, 159–167. https://doi.org/10.1016/j.copbio.2014.01.018

Harbaugh, A. W. (2005). *MODFLOW-2005, the US Geological Survey modular ground-water model: the ground-water flow process*, US Department of the Interior, US Geological Survey Reston.

Jiang, X.-W., Wan, L., Wang, X.-S., Ge, S., & Liu, J. (2009). Effect of exponential decay in hydraulic conductivity with depth on regional groundwater flow. *Geophysical Research Letters*, *36*, L24402. https://doi.org/10.1029/2009GL041251

Karimov, A. K., Šimůnek, J., Hanjra, M. A., Avliyakulov, M., & Forkutsa, I. (2014). Effects of the shallow water table on water use of winter wheat and ecosystem health: Implications for unlocking the potential of groundwater in the Fergana Valley (Central Asia). *Agricultural Water Management*, *131*, 57–69. https://doi.org/10.1016/j.agwat.2013.09.010

Koirala, S., Jung, M., Reichstein, M., de Graaf, I. E. M., Camps-Valls, G., Ichii, K., et al. (2017). Global distribution of groundwater-vegetation spatial covariation. *Geophysical Research Letters*, *44*, 4134–4142. https://doi.org/10.1002/2017GL072885

Lam, A., Karssenberg, D., van den Hurk, B. J. J. M., & Bierkens, M. F. P. (2011). Spatial and temporal connections in groundwater contribution to evaporation. *Hydrology and Earth System Sciences*, *15*(8), 2621–2630. https://doi.org/10.5194/hess-15-2621-2011

Li, X., Cheng, G., Ge, Y., Li, H., Han, F., Hu, X., et al. (2018). Hydrological cycle in the Heihe River Basin and its implication for water resource management in endorheic basins. *Journal of Geophysical Research: Atmospheres*, *123*, 890–914. https://doi.org/10.1002/2017JD027889

Li, X., Cheng, G., Lin, H., Cai, X., Fang, M., Ge, Y., et al. (2018). Watershed system model: The essentials to model complex human-nature system at the river basin scale. *Journal of Geophysical Research: Atmospheres*, *123*, 3019–3034. https://doi.org/10.1002/2017JD028154

Li, X., Liu, S., Xiao, Q., Ma, M., Jin, R., Che, T., et al. (2017). A multiscale dataset for understanding complex eco-hydrological processes in a heterogeneous oasis system. *Scientific Data*, *4*, 170083. https://doi.org/10.1038/sdata.2017.83

Li, X., Zheng, Y., Sun, Z., Tian, Y., Zheng, C., Liu, J., et al. (2017). An integrated ecohydrological modeling approach to exploring the dynamic interaction between groundwater and phreatophytes. *Ecological Modelling*, *356*, 127–140. https://doi.org/10.1016/j.ecolmodel.2017.04.017

Liu, C., Liu, J., Hu, Y., Wang, H., & Zheng, C. (2016). Airborne thermal remote sensing for estimation of groundwater discharge to a river. *Groundwater*, *54*(3), 363–373. https://doi.org/10.1111/gwat.12362

Loucks, D. P., Van Beek, E., Stedinger, J. R., Dijkman, J. P., & Villars, M. T. (2005). *Water resources systems planning and management: An introduction to methods, models and applications*. Paris: UNESCO.

Markstrom, S. L., Niswonger, R. G., Regan, R. S., Prudic, D. E., & Barlow, P. M. (2008). GSFLOW-Coupled Ground-water and Surface-water FLOW model based on the integration of the Precipitation-Runoff Modeling System (PRMS) and the Modular Ground-Water Flow Model (MODFLOW-2005), *Rep. 2328–7055* Geological Survey (US).

Markstrom, S. L., Regan, R. S., Hay, L. E., Viger, R. J., Webb, R. M., Payn, R. A., & LaFontaine, J. H. (2015). PRMS-IV, the precipitation-runoff modeling system, version 4, *Rep. 2328–7055*, US Geological Survey.

Miguez-Macho, G., & Fan, Y. (2012a). The role of groundwater in the Amazon water cycle: 1. Influence on seasonal streamflow, flooding and wetlands. *Journal of Geophysical Research*, *117*, D15113. https://doi.org/10.1029/2012JD017539

Miguez-Macho, G., & Fan, Y. (2012b). The role of groundwater in the Amazon water cycle: 2. Influence on seasonal soil moisture and evapotranspiration. *Journal of Geophysical Research*, *117*, D15114. https://doi.org/10.1029/2012JD017540

Pérez Hoyos, I. C., Krakauer, N. Y., Khanbilvardi, R., & Armstrong, R. A. (2016). A review of advances in the identification and characterization of groundwater dependent ecosystems using geospatial technologies. *Geosciences*, *6*(2), 17. https://doi.org/10.3390/geosciences6020017

Pokhrel, Y. N., Fan, Y., Miguez-Macho, G., Yeh, P. J. F., & Han, S.-C. (2013). The role of groundwater in the Amazon water cycle: 3. Influence on terrestrial water storage computations and comparison with GRACE. *Journal of Geophysical Research: Atmospheres*, *118*, 3233–3244. https://doi.org/10.1002/jgrd.50335

Qin, D., Qian, Y., Han, L., Wang, Z., Li, C., & Zhao, Z. (2011). Assessing impact of irrigation water on groundwater recharge and quality in arid environment using CFCs, tritium and stable isotopes, in the Zhangye Basin, Northwest China. *Journal of Hydrology*, *405*(1–2), 194–208. https://doi.org/10.1016/j.jhydrol.2011.05.023

Richardson, S., Ervine, E., Froend, R., Boon, P., Barber, S., & Bonneville, B. (2011). Australian groundwater-dependent ecosystem toolbox: Part 1: Assessment Framework, Waterlines Report*Rep*.

Scanlon, B. R., Keese, K. E., Flint, A. L., Flint, L. E., Gaye, C. B., Edmunds, W. M., & Simmers, I. (2006). Global synthesis of groundwater recharge in semiarid and arid regions. *Hydrological Processes*, *20*(15), 3335–3370. https://doi.org/10.1002/hyp.6335

Scanlon, B. R., Reedy, R. C., Stonestrom, D. A., Prudic, D. E., & Dennehy, K. F. (2005). Impact of land use and land cover change on groundwater recharge and quality in the southwestern US. *Global Change Biology*, *11*(10), 1577–1593. https://doi.org/10.1111/j.1365-2486.2005.01026.x

Tamea, S., Laio, F., Ridolfi, L., D'Odorico, P., & Rodriguez-Iturbe, I. (2009). Ecohydrology of groundwater-dependent ecosystems: 2. Stochastic soil moisture dynamics. *Water Resources Research*, *45*, W05420. https://doi.org/10.1029/2008WR007293

Taylor, R. G., Todd, M. C., Kongola, L., Maurice, L., Nahozya, E., Sanga, H., & MacDonald, A. M. (2012). Evidence of the dependence of groundwater resources on extreme rainfall in East Africa. *Nature Climate Change*, *3*(4), 374–378. https://doi.org/10.1038/nclimate1731

Tian, Y., Zheng, Y., Wu, B., Wu, X., Liu, J., & Zheng, C. (2015). Modeling surface water-groundwater interaction in arid and semi-arid regions with intensive agriculture. *Environmental Modelling & Software*, *63*, 170–184. https://doi.org/10.1016/j.envsoft.2014.10.011

Tian, Y., Zheng, Y., Zheng, C., Xiao, H., Fan, W., Zou, S., et al. (2015). Exploring scale-dependent ecohydrological responses in a large endorheic river basin through integrated surface water-groundwater modeling. *Water Resources Research*, *51*, 4065–4085. https://doi.org/10.1002/2015WR01688

Wilson, J. L., & Guan, H. (2004). Mountain-block hydrology and mountain-front recharge. *Groundwater recharge in a desert environment: The Southwestern United States*, 113–137.

Yao, Y., Huang, X., Liu, J., Zheng, C., He, X., & Liu, C. (2015). Spatiotemporal variation of river temperature as a predictor of groundwater/surface-water interactions in an arid watershed in China. *Hydrogeology Journal*, *23*(5), 999–1007. https://doi.org/10.1007/s10040-015-1265-y

Yao, Y., Zheng, C., Andrews, C., Zheng, Y., Zhang, A., & Liu, J. (2017). What controls the partitioning between baseflow and mountain block recharge in the Qinghai-Tibet Plateau? *Geophysical Research Letters*, *44*, 8352–8358. https://doi.org/10.1002/2017GL074344

Yao, Y., Zheng, C., Liu, J., Cao, G., Xiao, H., Li, H., & Li, W. (2014). Conceptual and numerical models for groundwater flow in an arid inland river basin. *Hydrological Processes*, *29*(6), 1480–1492. https://doi.org/10.1002/hyp.10276

Yao, Y., Zheng, C., Tian, Y., Li, X., & Liu, J. (2017). Eco-hydrological effects associated with environmental flow management: A case study from the arid desert region of China. *Ecohydrology*, *11*(1), e1914. https://doi.org/10.1002/eco.1914

Yao, Y., Zheng, C., Tian, Y., Liu, J., & Zheng, Y. (2014). Numerical modeling of regional groundwater flow in the Heihe River Basin, China: Advances and new insights. *Science China Earth Sciences*, *58*(1), 3–15. https://doi.org/10.1007/s11430-014-5033-y

Yeh, P. J. F., & Famiglietti, J. S. (2009). Regional groundwater evapotranspiration in Illinois. *Journal of Hydrometeorology*, *10*(2), 464–478. https://doi.org/10.1175/2008jhm1018.1

Zhao, J., Wang, X., & Wan, L. (2011). Runoff change and its simulation in main stream of heihe river at gaoya section. *Journal of Desert Research*, *5*, 043.